Macromolecules

Article

pubs.acs.org/Macromolecules



# Initiators Based on Benzaldoximes: Bimolecular and Covalently Bound Systems

Markus Griesser,[†] Arnulf Rosspeintner,[†,⊥] Claudia Dworak,[‡] Michael Höfer,[‡] Gottfried Grabner,[§] Robert Liska,[‡] and Georg Gescheidt*[,†]

[†]Institute of Physical and Theoretical Chemistry, Graz University of Technology, Stremayrgasse 9, 8010 Graz, Austria

[‡]Institute of Applied Synthetic Chemistry, Vienna University of Technology, Getreidemarkt 9/163/MC, 1060 Vienna, Austria

[§]Max F. Perutz Laboratories, University of Vienna, Campus-Vienna-Biocenter 5, 1030 Vienna, Austria

Supporting Information

**ABSTRACT:** Typical bimolecular photoinitiators (PIs) for radical polymerization of acrylates show only poor photoreactivity because of the undesired effect of back electron transfer. To overcome this limitation, PIs consisting of a benzaldoxime ester and various sensitizers based on aromatic ketones were introduced. The core of the photoinduced reactivity was established by laser flash photolysis, photo-CIDNP, and EPR experiments at short time scales. According to these results, the primarily formed iminyl radicals are not particularly active. The polymerization is predominantly initiated by C-centered radicals. Photo-DSC experiments show reactivities comparable to that of classical monomolecular type I PIs like Darocur 1173.

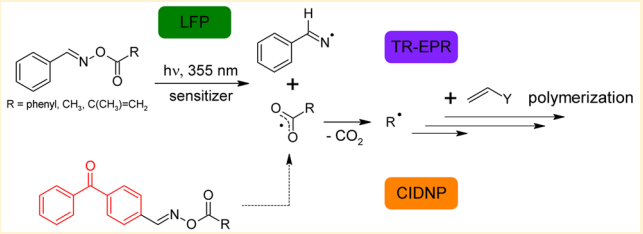


## INTRODUCTION

Photocuring is the key technique for the preparation of films and coatings as it offers a broad and economic application spectrum for industry.[1] During the curing process, the photoinitiator (PI) plays the decisive role. It absorbs energy from a photon either in a direct or an indirect process, transferring it into chemical energy. After the excitation process a reactive radical can be formed, which is able to induce the polymerization of a wide range of monomers. Among the bimolecular type II PIs for radical photopolymerization, excitable chromophores like benzophenone in combination with tertiary amines as co-initiators are commonly applied.[2] The ketone−amine interactions proved to be highly efficient concerning radical formation due to electron transfer. The efficiency of the photochemical process depends on the rate constant of electron and proton transfer as well as the reactivity of the $\alpha$-amino alkyl radical toward reactive double bonds and quenching by side reactions.[3] A wide range of co-initiators have been investigated such as different aliphatic and aromatic amines.[4,5] Thiols[6] and Si−H groups[7] are also described as efficient co-initiators in the literature, but only limited storage stability is given for such formulations.

Unfortunately, the efficiency of this system is usually reduced by back electron transfer (BET), the solvent cage effect, and limited diffusion capability in highly viscous formulations or water-based systems.[8] Molecular oxygen from the atmosphere easily inhibits the polymerization process. Consequently, PI systems, which are unperturbed by oxygen are preferred because it is unfavorable to work under a nitrogen atmosphere. Using *N*-phenylglycine as co-initiator for benzophenone, the decarboxylation step delivers enough $CO_2$ to displace $O_2$ from the curing material.[9,10] Recently, a very efficient class of PIs has been created by covalently linking benzophenone and *N*-phenylglycine, thus keeping the co-initiator in close proximity.[8,11]

Also, oxime esters might produce $CO_2$ after cleavage of the N−O bond and decarboxylation of the acyloxy radical. Accordingly, this type of functional group in combination with photosensitizers was considered as an alternative concept for type II initiator systems. Several investigations on the photolysis of *O*-acyl oximes in the presence of photosensitizers can be found in the literature.[12,13] Yoshida et al.[14] described the nature of the triplet states and the subsequent photochemistry of aromatic *O*-acyl oximes. They postulated a requirement of close triplet state energies of the oximes ($E_T$ = 289−305 kJ mol$^{-1}$) and their ketone-based sensitizers, displaying a $\pi-\pi^*$ character. The excitation energies are dissipated by cleavage of the N−O bond. Moreover, the photolysis of aldoxime esters in presence of a sensitizer like 4-methoxyacetophenone was investigated by McCarroll and Walton, performing EPR measurements and radical trapping experiments, thus presenting a new class of radical precursors for spectroscopic studies (Scheme 1).[15]

Furthermore, such sensitized *O*-acyloximes were tested in a patent,[16] but unfortunately no exact data on their performance was given. Structure related $\alpha$-keto-*O*-acyloximes[17] have found

**Received:** September 19, 2012
**Revised:** October 8, 2012
**Published:** November 1, 2012

  

**Scheme 1. Photochemistry of (Sensitized) Aldoximes**

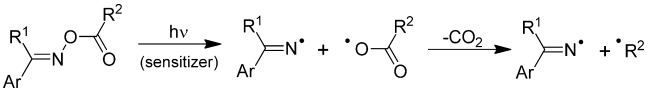


specialized industrial applications, such as color filter resists, however, thermal stability of such compounds is always crucial.[18] Very recently, we have investigated some benzaldoxime esters in combination with 4-methylbenzophenone as sensitizer and have found surprisingly high photoreactivity in photo-DSC experiments.[19]

Therefore, it was of interest to investigate the initial reactions of this photoinitiator system in more detail by laser flash photolysis experiments, photo-CIDNP, and EPR measurements. Photo-DSC experiments allow the comparison of these new systems with established photoinitiators.

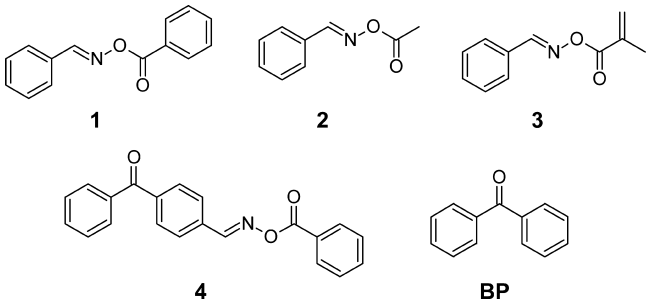


**Figure 1.** Benzaldoxime esters and the employed sensitizer.

## EXPERIMENTAL SECTION

All reagents were purchased from Sigma-Aldrich and were used without further purification. **HDDA** and 2-hydroxy-2-methyl-1-phenyl-1-propanone (Darocur 1173; **D1173**) were received as a gift from Ivoclar Vivadent and BASF, respectively. The solvents were dried and purified by standard laboratory methods. The synthesis of benzaldoxime esters **1**–**4** has recently been published.[19]

Nanosecond transient absorption spectroscopy was carried out using the third harmonic (355 nm) of a Q-switched Nd:YAG laser (Spectra-Physics LAB-150) with a pulse duration of 8 ns. Transient absorbances were measured in a right-angle setup using a cell holder with incorporated rectangular apertures defining a reaction volume of dimensions 0.17 cm (height), 0.32 cm (width), and 0.13 cm (depth) within the cell. Pulse energies between 0.1 and 4 mJ/pulse were used, the typical value for the measurement of transient spectra being 2 mJ/pulse. Pulse energies were measured using a ballistic calorimeter (Raycon-WEC 730). Solutions were deoxygenated by bubbling with argon. Further details of experimental procedures have been published previously.[20]

Time-resolved continuous-wave electron paramagnetic resonance (CW TR-EPR) experiments were performed using a frequency-tripled Nd:YAG laser (Continuum Surelite II, 20 Hz repetition rate; 355 nm; ca. 10 mJ/pulse; ca. 10 ns), a Bruker ESP 300E X-band spectrometer (unmodulated static magnetic field), and a LeCroy 9400 dual 125 MHz digital oscilloscope. The TR-EPR spectrum is obtained by scanning the desired magnetic field range recording the accumulated (usually 50–100 accumulations) EPR time responses to the incident laser pulses at a given static magnetic field. The system is controlled using a program developed, kindly provided and maintained by Dr. J. T. Toerring (Berlin, Germany). Argon-saturated solutions were pumped through a quartz tube (inner diameter 2 mm, flow ca. 2–3 mL/min) in the rectangular cavity of the EPR spectrometer. The samples were 10 mM in benzaldoxime and benzophenone, while—when added—0.15 M in butyl acrylate. The EPR spectra were simulated using the Easyspin package[21] for MATLAB (version 3.1.7).

The hyperfine coupling constants (hfcs) of the free radicals were calculated using the Gaussian03 package.[22] All calculations (geometry optimizations and single point calculations) were conducted at the B3LYP[23,24] level of theory with the basis set TZVP.[25]

Photo-CIDNP experiments were performed on a 200 MHz Bruker AVANCE DPX spectrometer. Irradiation was carried out using a frequency-tripled Spectra-Physics Nd:YAG INDI laser (355 nm, ca. 40 mJ/pulse, ca. 10 ns). The following pulse sequence was used: presaturation–laser flash–30° RF detection pulse (2.2 $\mu$s)–free induction decay. The concentrations of the initiators were typically 0.01 M in $d_3$-acetonitrile or $d_6$-benzene, deaerated by bubbling argon through the solution.

DSC photocuring experiments were carried out in HDDA with 0.12 $\mu$M of each component (~2 wt % of **1**) under a nitrogen atmosphere, using an EXFO Omnicure 2001 UV lamp with a 200–500 nm filter and a Netzsch DSC 204 F1 Phoenix with autosampler.

## RESULTS

**Laser Flash Photolysis.** Nanosecond transient absorption spectroscopy of solutions of benzophenone and the co-initiating *O*-acyloximes **1** and **2** as well as solutions of the covalently bound *O*-acyloxime **4** was used to gain information on the early photochemical steps. In case of the co-initiating oximes, the experiments were performed in deaerated MeCN in equimolar ($5 \times 10^{-3}$ and $1 \times 10^{-2}$ M) and different concentrations of sensitizer **BP** ($1 \times 10^{-2}$ M) and oxime ($1 \times 10^{-3}$ M), respectively. The irradiation wavelength (355 nm) exclusively excites benzophenone chromophores into the n, $\pi^*$ state.[26]

Upon irradiation of solutions **BP**/**1** and **BP**/**2**, as expected, the first transient appearing at the nanosecond time scale was the characteristic benzophenone triplet–triplet absorption around 520 nm. At a longer time scale, several additional absorption bands emerged. However, the microsecond-range lifetimes of these transients suggested that they originated from radical-type precursors. The degradation kinetics of the benzophenone triplet ($\mathbf{BP}^T$) in the conducted experiments under variation of sensitizer and co-initiating oxime concentrations gave no indication of ground-state complex formation. Regarding transients originating from $\mathbf{BP}^T$, no traces of benzophenone ketyl radicals or radical anions could be detected. Because of the lack of product species originating from H abstraction reactions or electron transfer processes, the sensitization presumably proceeds via an efficient energy transfer.[14,27]

In contrast to the co-initiating systems **BP**/**1** and **BP**/**2**, no local triplet state of the benzophenone moiety was detectable in the photolysis of covalently bound benzophenone–*O*-acyloxime **4**. Here the sensitization process is successfully shifted from a diffusion-controlled, bimolecular process to an intramolecular energy transfer due to the spatial arrangement of the chromophore system and the oxime moiety. As a result of this fundamental change in the sensitization mechanism, the triplet lifetime is shortened to an extent ($\tau < 5$ ns) that is no longer directly assessable by the time resolution of our laser flash photolysis setup. Nevertheless, other transient absorption bands on a longer time scale remained completely identical.

In regard to possible primary cleavage products in the photolysis of the co-initiating *O*-acyloxime **1**, a transient subsequent to triplet states on the nanosecond time scale obviously originates from the triplet $\mathbf{BP}^T$. The visible spectrum of this transient (**6**) exhibited a slow but continuous progress of


dx.doi.org/10.1021/ma301959n | *Macromolecules* 2012, 45, 8648–8657

absorption in minor intensity from below 550 nm up to and above 800 nm, resembling the absorption of the benzoyloxyl radical obtained by photolysis of dibenzoyl peroxide.[28] In case of the oxime **2**, which should produce a less stable alkoyloxyl radical, an analogue transient to **6** could not be detected. The degradation of the triplet $\mathbf{BP}^T$ at 530 nm and the buildup of the absorption of **6** at 830 nm in the photolysis of *O*-acyloxime **1** are illustrated in Figure 2. The kinetic congruence between both traces is a strong indication that the benzophenone triplet $\mathbf{BP}^T$ is the precursor of the benzoyloxyl radical **6**.

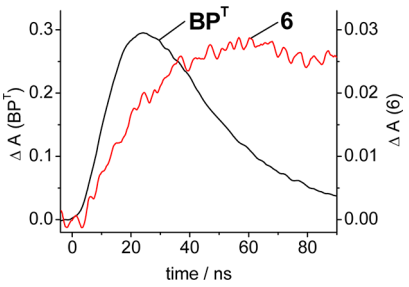


**Figure 2.** Temporal absorbance change of $\mathbf{BP}^T$ at 530 nm and **6** at 830 nm upon 355 nm laser flash photolysis of an equimolar solution of benzophenone and the *O*-acyloxime **1** in MeCN ($1 \times 10^{-2}$ M).

Unfortunately, **6** displays a low extinction coefficient in the accessible wavelength range, and related values given in the literature vary significantly.[29,30] Consequently, a reliable estimation of the quantum yield is not possible. Nevertheless, the yield of the benzoyloxyl radical **6** was determined as the product $\varepsilon_{830} \times \Phi(\mathbf{6})$ in an equimolar solution of **1** and benzophenone in MeCN ($1 \times 10^{-2}$ M). The results are shown in Figure 3 in the form of the absorbance of $\mathbf{BP}^T$ at 530 nm and **6** at 830 nm, versus the energy of the laser pulse.

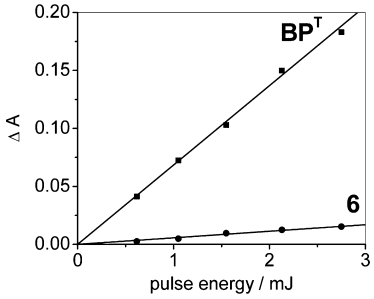


**Figure 3.** Absorption of $\mathbf{BP}^T$ at 530 nm obtained at 20 ns and **6** at 830 nm at 50 ns after 355 nm laser flash photolysis of an equimolar solution of benzophenone and the *O*-acyloxime **1** in MeCN ($1 \times 10^{-2}$ M) as a function of laser pulse energy.

The dependence determined for both the yield of triplet benzophenone $\mathbf{BP}^T$ and benzoyloxyl radical **6** is linear. The value of the product $\varepsilon_{830} \times \Phi(\mathbf{6})$ in MeCN was found to be 200 $M^{-1}$ $cm^{-1}$. Additionally, an important conclusion that can be drawn from this experiment is that the formation process is purely monophotonic.

In the photo-DSC experiments[19] the co-initiating oximes **1** and **2** displayed a higher activity as PIs compared to the covalently bound *O*-acyloxime **4**. Therefore, two different conclusions are possible: PI activity of **4** is reduced due to (1) a reduction of quantum yield for the cleavage or (2) a less reactive initiating species produced. In nanosecond transient absorption spectroscopy, the covalently bound *O*-acyloxime **4** yields a transient, which is completely congruent to the benzoyloxyl radical **6** but shows accelerated buildup kinetics. Apart from the differences in sensitization, **4** follows an analogue photodegradation chain as **1**. However, in comparison to the co-initiating oxime **1**, the product $\varepsilon_{830} \times \Phi(\mathbf{6})$ is approximately halved. Thus, the spatial arrangement of the benzophenone and oxime moieties in the structure of **4** causes a reduction in radical quantum yield in comparison to the co-initiating system.

It must be assumed that the benzoyloxyl radical **6** is produced by a homolytic scission of the N−O bond upon photolysis of **4** and **1**. Consequently, this type of photodegradation should result in the formation of an iminyl radical. Nevertheless, no transient absorption in the measured wavelength range (300−840 nm) could be assigned to a primary formed iminyl radical. Since iminyl radicals are rarely reported in the literature as transients in laser flash photolysis, it can be reasonably argued that this species shows no or an insufficient absorbance for a detection in the applied analytical setting.

Apart from primary photolysis products, secondary radicals appear as subsequent transients at the nanosecond time scale in the photolysis of all *O*-acyloxime PIs. These transients possess absorptions between 350 and 500 nm and resemble adducts of benzoyloxyl radicals to aromatic rings as described in the literature.[28,31] The degradation of the benzoyloxyl radical **6** at 830 nm and the buildup of one of these transients ($\mathbf{T}_1^{add}$) at 390 nm in the photolysis of *O*-acyloxime **1** are illustrated in Figure 4. The kinetic resemblance between the traces is another strong indication that the benzoyloxyl radical **6** is the precursor of the secondary adduct $\mathbf{T}_1^{add}$ (see Scheme 2).

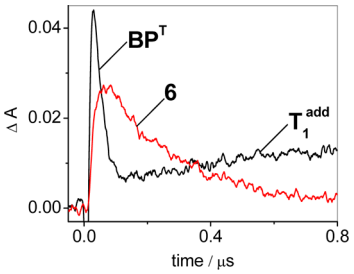


**Figure 4.** Temporal absorbance change of $\mathbf{BP}^T$ and $\mathbf{T}_1^{add}$ at 390 nm and **6** at 830 nm upon 355 nm laser flash photolysis of an equimolar solution of benzophenone and the *O*-acyloxime **1** in MeCN ($1 \times 10^{-2}$ M).

The decay of the transient **6**, as shown in Figure 4, proceeded with a first-order rate constant $k_1 = 4 \times 10^6$ $s^{-1}$. This rate has to be regarded as the product of a superposition of two well-known concurrent reactions: the first-order decarboxylation process after escape from the solvent cage and the pseudo-first-order addition to aromatic structures of the photolysis solution. The trace of $\mathbf{T}_1^{add}$ in Figure 4 is partially distorted due to a spectral overlap by at least a second, similar benzoyloxyl radical adduct $\mathbf{T}_2^{add}$ which exhibits different degradation kinetics. In contrast to $\mathbf{T}_1^{add}$, an adduct transient which resembles $\mathbf{T}_2^{add}$ was also detected in the photolysis of *O*-acyloxime **4**. In the case of the covalently bound *O*-acyloxime, the congruence between the degradation of the benzoyloxyl radical and the buildup kinetics of $\mathbf{T}_2^{add}$ could be more easily studied since no overlap with a triplet spectrum occurs. In the photolysis of the co-initiating *O*-


dx.doi.org/10.1021/ma301959n | *Macromolecules* 2012, 45, 8648−8657

**Scheme 2. Cleavage Mechanism of the BP/1 System and the Follow-up Transients (Ar = Substituted Aromatic Fragment, Derived from the Starting Compounds) Identified by LFP**

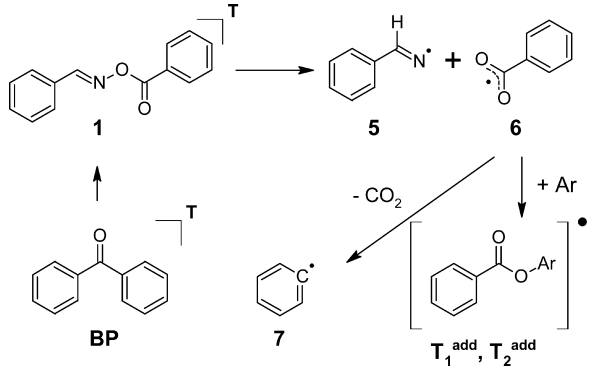


acyloxime **2**, which produces an alkoyloxyl radical, the relative absorbance of transients comparable to $T_1^{add}$ or $T_2^{add}$ is significantly lower. This is the logical consequence of an acceleration of the concurrent reaction, the decarboxylation of the less stable alkoyloxyl radical.

**Magnetic Resonance.** To obtain insight into the early stages of polymerizations, continuous-wave TR-EPR and $^1$H CIDNP experiments were performed. Both methods yield complementary results. Via EPR one is able to establish the radicals formed within the first 50 ns after irradiation,[32,33] whereas using CIDNP one can gain information about the products formed via the primary radical pair.[34,35] As the general model, the system **BP/1** was investigated by both TR-EPR and $^1$H CIDNP. Additionally, we present $^1$H CIDNP results for **BP/2**, **BP/3**, and **4**.

**TR-EPR.** Upon irradiation of a mixture of **BP** (10 mM) and **1** (10 mM) in acetonitrile in an EPR spectrometer, employing a 355 nm pulsed light source, the time-resolved EPR spectrum shown in Figure 5 (lower panel) is recorded. All signals appear in absorption with similar signal intensities in the low- and high-field portions of the spectrum, indicating that the radicals are formed via the triplet mechanism.[36] The two primary radicals formed by homolytic N−O bond cleavage of **1** can be easily identified. The nitrogen-centered radical **5** dominates the spectrum and is characterized by two triplets centered at 338.2 mT. The benzoyloxyl radical **6** gives rise to a broad peak at 336.8 mT, with a high *g* value characteristic for oxygen-centered radicals. Additional signals stemming from phenyl radical **7** in the center of the spectrum are shown in Figure 6. From the associated time traces it can be inferred that **6** produces **7** via decarboxylation within about 500 ns. The extracted hyperfine coupling constants (hfcs) for **7** are in agreement with published data[37] and calculations (see Figure 8). No signals stemming from (reduced) **BP** or related radicals could be identified, again indicating that **BP** only acts as a sensitizer.

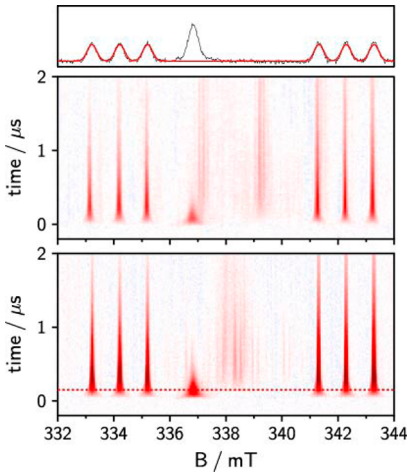


**Figure 5.** TR-EPR spectrum of a solution of **1** (10 mM) and **BP** (10 mM) in acetonitrile in the absence (lower panel) and presence (upper panel) of 0.1 M butyl acrylate. The upmost panel represents the spectrum at the time delay (150 ns) indicated by the dashed red line in the 3D spectrum, showing the nitrogen-centered radical (and its simulation) as well as the benzoyloxyl radical.

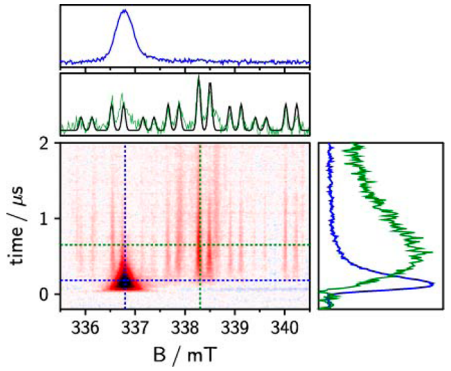


**Figure 6.** Zoom-in on the central part of the TR-EPR spectrum shown in Figure 5 in the absence of butyl acrylate. For better visibility of the low intensity radical **7** signals the color map was cut at values far below the maximum of the radical **6** signal maximum. The blue and green spectra and time traces are cuts along the field and time axis at values indicated by the colored dashed lines.

To study the time profiles of the addition of radicals to monomers, butyl acrylate (**BA**) was added to the **BP/1** system. Upon this addition (EPR spectrum in Figure 5, upper panel) one can immediately see that the time evolution of radicals **5** and **6** is hardly affected. But a change in the signal pattern of the central part of the spectrum can be clearly discerned (Figure 7). In the presence of 0.1 M **BA**, **7** vanishes and gives rise to a new signal, which can be assigned to the addition product of phenyl radical **7** to **BA**, **7-BA**. No direct hyperfine data for the adduct **7-BA** could be found in the literature, but EPR data for the addition of phenyl radicals to methyl acrylate[38] and benzoyl radicals to **BA**[39] as well as theoretical calculations are in agreement with this assignment.

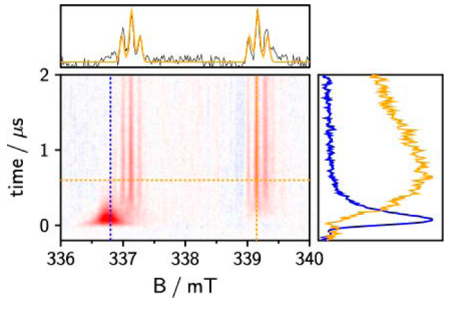


**Figure 7.** Zoom-in on the central part of the TR-EPR spectrum shown in Figure 5 in the presence of butyl acrylate (0.1 M). The 2D spectrum and time traces are obtained by cuts along the axis at the indicated colored dashed lines.


dx.doi.org/10.1021/ma301959n | *Macromolecules* 2012, 45, 8648−8657

Thus, we were able to establish the primary radicals formed directly upon photolysis of **1** by TR-EPR. By the addition of **BA** it could be shown that there is no reactivity of the nitrogen-centered iminyl radical **5** toward the monomer in the observed time scale. Additionally decarboxylation of **6** toward **7** is fast enough that no addition of **6** to **BA** could be discerned from the spectra. The addition of phenyl radicals **7** to **BA** is fast enough to repress the EPR signal of **7** (Figure 7).

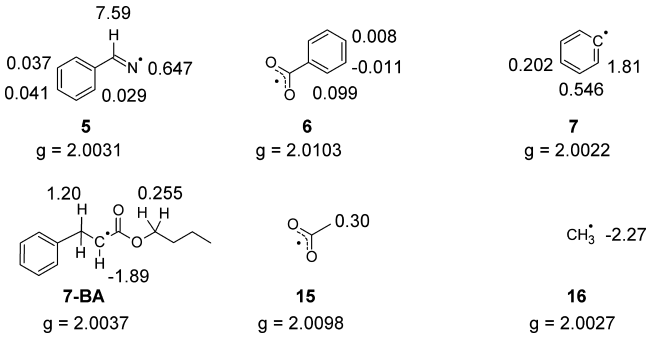


**Figure 8.** Calculated hyperfine coupling constants and *g* factors (B3LYP/TZVP).

**Table 1. Hyperfine and *g* Value Data Extracted from TR-EPR Spectra**

| radical | *g* value | hfc/mT |
|---|---|---|
| **5** | 2.0017 | 0.99 (N,1)/8.08 (H,1) |
| **6** | 2.0103 | <1 |
| **7** | 2.0012 | 1.74 (H,2)/0.62 (H,2)/0.23 (H,1) |
| **7** (ref 37) | 2.0023 | 1.743 (H,2)/0.625 (H,2)/0.204 (H,1) |
| **7-BA** | 2.0025 | 2.04 (H,1)/2.18 (H,2)/0.16 (H,2) |

**CIDNP.** Initially experiments irradiating only the benzaldoxime esters **1**, **2**, and **3** were performed. Except for some small polarized signals of parent compounds, no reaction products could be discerned, reflecting the necessity of a photosensitizer.

As the reference experiment, the mixture benzophenone **BP**/benzaldoxime benzoate **1** was photolyzed inside the NMR spectrometer. The NMR spectrum before irradiation (see Figure 9a) shows a distinct signal for the aldoxime hydrogen at $\delta$ = 8.70 ppm. The rest of the spectrum is made up of two separated groups in the aromatic region the one with the higher shift ($\delta$ = 8.09−8.15 ppm) stemming from the protons of the benzoate moiety. The signals of **BP** as well as the other aromatic hydrogens of **1** make up the rest of the spectrum.

The polarization effect of CIDNP can occur in absorption and emission. It is caused by an interaction of the electron and nuclear spin in the radical pair. Therefore, the determining factors to the effect are the sign and magnitude of the radicals' magnetic properties (*g* value, hyperfine, and *J* coupling) as well as the initial spin state and the reaction pathway ("cage" or "escape" product). The resulting CIDNP signals can easily be rationalized employing Kaptein's rules.[40]

Immediately after irradiation using a single Nd:YAG laser pulse, a CIDNP spectrum was recorded (see Figure 9b). It can be assigned as follows: The emissive peak at $\delta$ = 8.70 ppm corresponds to the reformation of parent compound **1**. A second emissive peak can be found at $\delta$ = 8.03 ppm, which is assigned to the *Z*-isomer **1i** of the parent compound (*E*-isomer), also generated by in "cage" recombination. The shift difference of $\Delta\delta$ = 0.67 ppm is characteristic for the two isomers.[41] Of the signals in absorption, benzene **13** at $\delta$ = 7.37 ppm has the highest intensity. It is generated by the decarboxylation of benzoyloxyl radical **6** to phenyl radical **7** and followed by hydrogen transfer from iminyl radical **5**, the most likely hydrogen donor (see Scheme 3). Benzonitril **8**, the byproduct of this reaction, is not distinguishable owing to its aromatic hydrogens stemming from iminyl radical **5** where they only had small hfcs, thus leading to low polarizations. The two absorptive signals at $\delta$ = 8.55 and 8.42 ppm can be assigned to the *E*- and *Z*-isomers of *N*-benzylideneaniline **11** and **12**, respectively. Those are formed from the recombination of phenyl radical **7** and iminyl radical **5**. The *E*-isomer displays higher signal intensity because it is the less sterically hindered

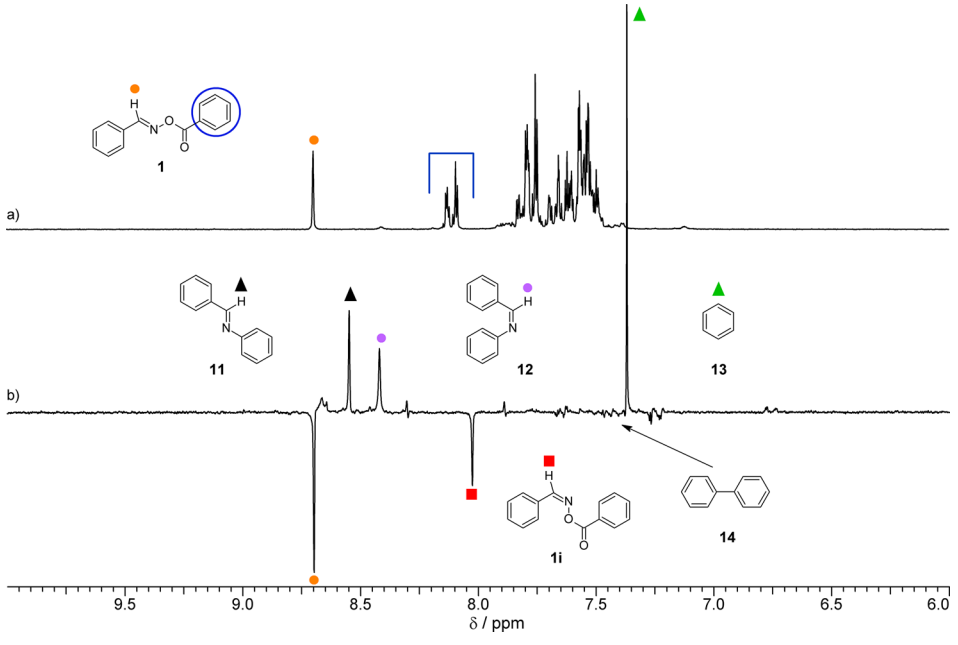


**Figure 9.** (a) $^1$H NMR spectrum of the mixture **BP**/**1**. (b) $^1$H CIDNP spectrum obtained immediately after the laser pulse (355 nm).


dx.doi.org/10.1021/ma301959n | *Macromolecules* 2012, 45, 8648−8657

**Scheme 3. Reaction Products Generated by Photolysis of the Mixture BP/1**

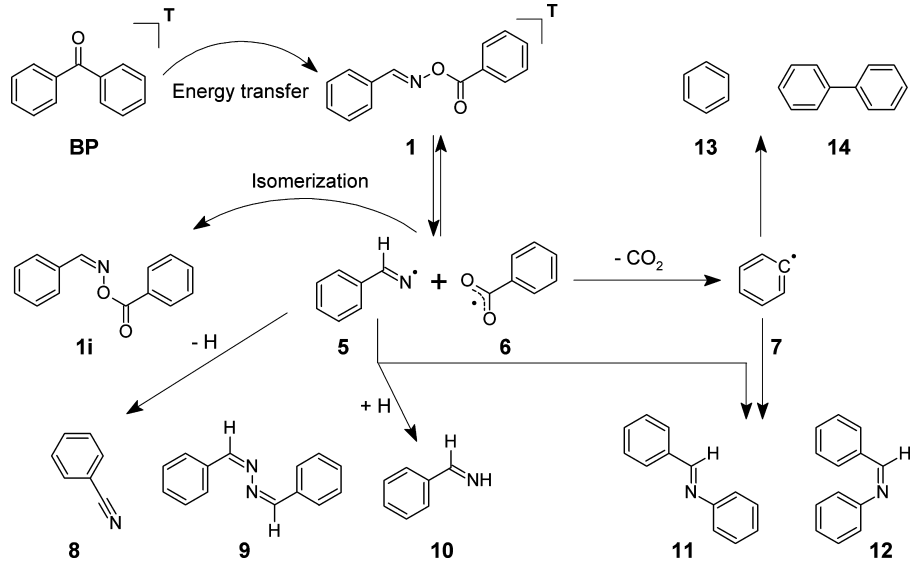


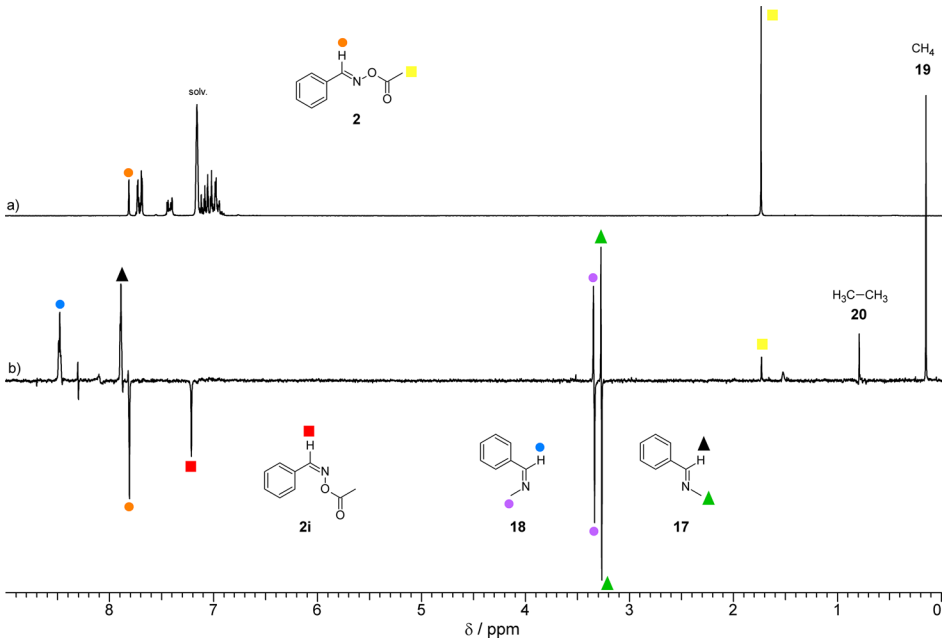


**Figure 10.** (a) $^1$H NMR spectrum of the mixture **BP/2**. (b) $^1$H CIDNP spectrum obtained immediately after the laser pulse (355 nm).

isomer. In addition, the *E*-isomer is thermodynamically favored leading to thermal isomerization of the *Z*-isomer.[42] There are also another few possibilities of recombination, which are indicated in Scheme 3. The recombination of two phenyl radicals **7** leads to biphenyl **14** which can be accommodated by the occurrence of small signals at around $\delta$ = 7.4 ppm. The low intensity is expected because the phenyl ring does not carry a lot of polarization in addition to **14** being an "escape" product. An "escape" recombination of two radicals **6** is not expected because of the fast decarboxylation reaction. An analogous recombination is likely for iminyl radical **5** leading to azine **9**. Radical **5** can also abstract a hydrogen (most likely from another **5**) and form benzaldimine **10**. The CIDNP spectra of **1**, **2**, and **3** are all expected to give identical follow-up products via radical **5**. This is corroborated by identical peaks at $\delta$ = 7.89 and 8.30 ppm in all three spectra. Substances **9** and **10** are therefore tentatively assigned to those peaks.

Benzaldoxime acetate **2** shows a similar behavior as **1**, except for the differing carbon-centered radical fragment. To avoid a signal overlap appearing in $d_3$-acetonitrile, the spectra of **2** were recorded in $d_6$-benzene. Except for solvent shifts, the reaction is compatible in both solvents. In the NMR spectrum (Figure 10a) of the mixture **BP/2** there are only two identifiable singlet peaks, namely the signal of the aldoxime hydrogen at $\delta$ = 7.81 ppm and the singlet of the methyl end group at $\delta$ = 1.73 ppm. The remaining signals stem from the aromatic hydrogens of both compounds, which are not individually attributable. The solvent signal is visible at $\delta$ = 7.16 ppm.

Upon irradiation of the solution (Nd:YAG laser - single pulse) there are more signals in the CINDP spectrum (Figure 10b) than in the case of **1**. There are signals in emission at $\delta$ = 7.81 and 7.21 ppm, which stem from recombination of the primary radicals **5** and **15** to the parent compound **2** and its isomer **2i**, respectively ($\Delta\delta$ = 0.60 ppm). The acetoyl radical **15**


dx.doi.org/10.1021/ma301959n | *Macromolecules* 2012, 45, 8648–8657

**Scheme 4. Reaction Products Generated by Photolysis of the Mixture BP/2**

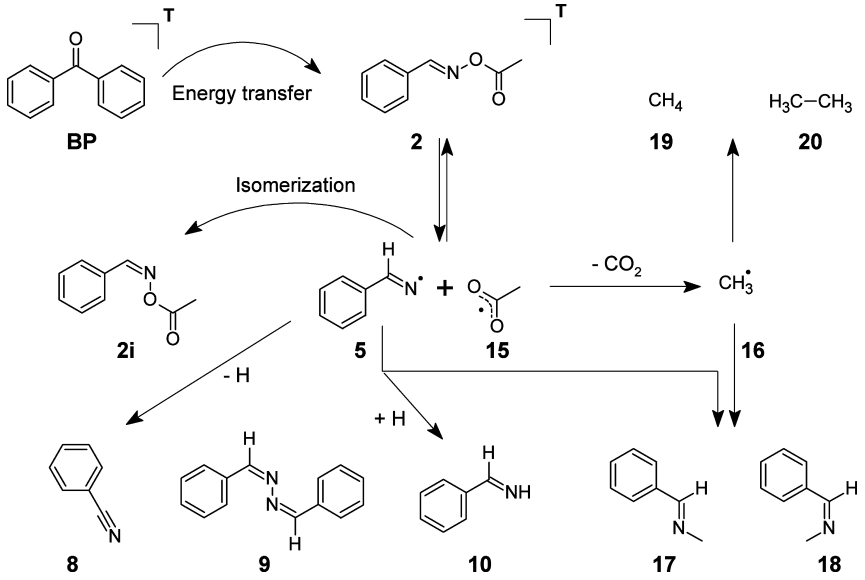


resulting from triplet cleavage of **2** undergoes decarboxylation generating methyl radical **16**. This radical can then take part in different recombination reactions. The first one is hydrogen transfer from radical **5**, which leads to methane **19** and can be found in absorption at $\delta$ = 0.15 ppm. As for **1**, benzonitrile **8** is a byproduct but is not clearly distinguishable in the spectrum. Another absorptive signal in the aliphatic region is found at $\delta$ = 0.79 ppm and can be assigned to the "escape" reaction of two methyl radicals forming ethane **20**. Moreover, the recombination of radicals **5** and **16** leads to the *E*- and *Z*-isomer of *N*-benzylidenemethanamine, **17** and **18**, respectively. The corresponding signals are two quadruplets at $\delta$ = 8.48 and 7.89 ppm as well as two doublets at $\delta$ = 3.35 and 3.27 ppm. Because these signals stem from coupled polarized protons, they both show the multiplet effect A/E (first absorption, then emission). This behavior, also described in Kaptein's rules,[40] is easily visible for the two methyl doublets. For the two iminyl quadruplets there is also overlying enhanced absorption; thus, only the latter peaks are visible in emission. The two isomers could be assigned using the $^4J$ coupling constant, which is known for the *E*-isomer ($^4J$ = −1.6 Hz).[43] Therefore, the signals at $\delta$ = 7.89 and 3.27 ppm belong to **17** ($^4J$ = −1.6 Hz) and the signals at $\delta$ = 8.48 and 3.35 ppm to **18** ($^4J$ = −2.2 Hz). Two other signals at $\delta$ = 8.31 and 7.82 ppm are assigned to substances **9** and **10** in analogy to **1** (see above). The slightly different shift values are caused by the different solvent ($d_6$-benzene vs $d_3$-acetonitrile).

Benzaldoxime methacrylate **3** shows the same behavior as esters **1** and **2**. But, contrary to the other substances investigated in this work, **3** features an end group including a reactive vinyl moiety, causing additional follow-up products and polarization effects.

The $^1$H NMR spectrum of **BP/3** shows the aldoxime hydrogen signal at $\delta$ = 8.56 ppm, and the protons of the aromatic ring are concentrated in the region $\delta$ = 7.44−7.81 ppm. Further features of the NMR spectrum are two multiplets at $\delta$ = 5.75 and 6.19 ppm assigned to the *E*- and *Z*-hydrogen of the vinyl bond, respectively. Additionally a multiplet stemming from the methyl group can be seen at $\delta$ = 2.01 ppm.

The $^1$H CIDNP spectrum shows typical features of recombination reactions of the initial radical pair of **5** and **21**, leading to polarized signals of parent **3** at $\delta$ = 8.56 ppm and of isomer **3i** at $\delta$ = 7.93 ppm ($\Delta\delta$ = 0.63 ppm). Also substances **9** and **10** appear in the spectrum as two polarized doublets at $\delta$ = 7.89 and 8.30 ppm. The iminyl hydrogens of products **23** and **24** stemming from recombination of radicals **5** and propen-2-yl radical **22** after decarboxylation can be found at $\delta$ = 8.32 and 8.11 ppm, respectively. There are some additional signals visible in this region, which are probably generated by additional recombination reactions of **5**. All the other fragmentation products lead to compounds containing one or more double bonds generating a number of polarized multiplets for vinyl and aliphatic hydrogens. For those it is impossible to discern the single components, owing to several overlapping resonances (see Supporting Information).

The unimolecular initiator **4** shows similar behavior and spectra as the bimolecular type **BP/1**. The $^1$H NMR spectrum (see Figure 11a) shows one isolated resonance signal at $\delta$ = 8.80 ppm stemming from the aldoxime hydrogen. The

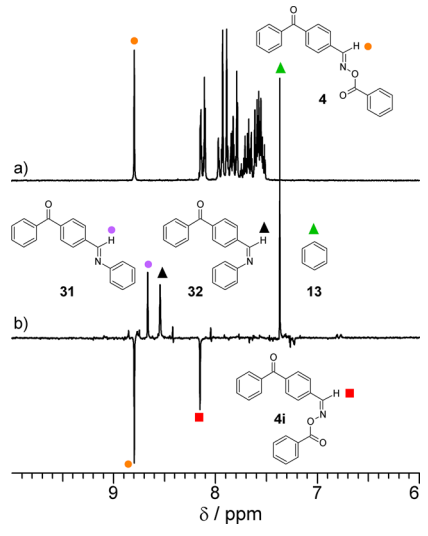


**Figure 11.** (a) $^1$H NMR spectrum of **4**. (b) $^1$H CIDNP spectrum obtained immediately after the laser pulse (355 nm).


dx.doi.org/10.1021/ma301959n | *Macromolecules* 2012, 45, 8648−8657

**Scheme 5. Reaction Products Generated by Photolysis of the Covalently Bound Initiator 4**

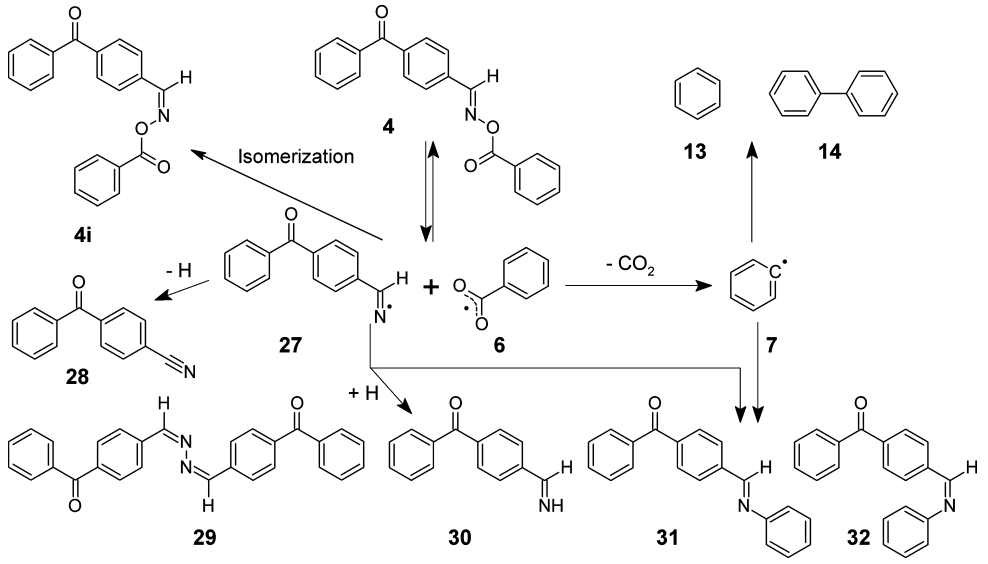


remaining protons of the molecule are attached to aromatic rings and occur as one block of signals ($\delta$ = 7.52−8.15 ppm).

Upon irradiation, the initiator **4** undergoes cleavage of the N−O bond analogous to **1** (see Laser Flash Photolysis section). The most prominent signal in the $^1$H CIDNP spectrum (Figure 11b) is benzene **13** at $\delta$ = 7.37 ppm in absorption generated via decarboxylation of benzoyloxyl radical **6**. The recombination isomer of **4** (emissive signal at $\delta$ = 8.80 ppm), **4i**, can be found in emission at $\delta$ = 8.15 ppm. The shift difference of $\Delta\delta$ = 0.65 ppm is in accordance with the isomerization of the other three molecules **1**−**3**. The two remaining absorptive signals are assigned to the recombination reactions of iminyl radical **27** and benzyl radical **7** after decarboxylation. In the same way as for the bimolecular system **BP**/**1**, the two *E*- and *Z*-isomers (**31** and **32**, respectively) can be found at $\delta$ = 8.67 and 8.54 ppm, **31** showing the higher intensity. Furthermore, signals stemming from biphenyl **14** can be seen at low intensity at the base of the benzene signal. There are also products **28**−**30**, analogous to **8**−**10** formed from the iminyl radical **5** stemming from **1**. The 4-cyanobenzophenone **28** did not show polarization in the CIDNP spectrum, but the peaks at $\delta$ = 8.05 and 8.42 ppm are tentatively assigned to **29** and **30**. The reaction mechanism can be found in Scheme 5.

To study the reactivity of the generated radicals toward monomers, CIDNP experiments were performed in the presence of two acrylates, butyl acrylate (**BA**) and 3,3-dimethyl-2-methylenebutanoate (***t*-BAM**), analogous to the TR-EPR measurements. The bulky *tert*-butyl substituent of ***t*-BAM** hampers the polymerization process and thus does not lead to a propagating polymer chain. This is desired, because it reduces the number of follow-up reactions and therefore the influence of the growing chain on the studied reactions can be followed. The molar ratio of initiator to monomer was in the range of 1:5−1:15.

It can be seen in Figure 12 that the addition of the monomer **BA** leads to an easily identifiable effect in the CIDNP spectrum. The benzene signal intensity is reduced by about 60%. A similar reduction of intensity can be seen for the two products **11** and **12**, which are recombination products formed after decarboxylation. This decrease also correlates with the initiator/monomer ratio. In contrast, the two emission peaks of the

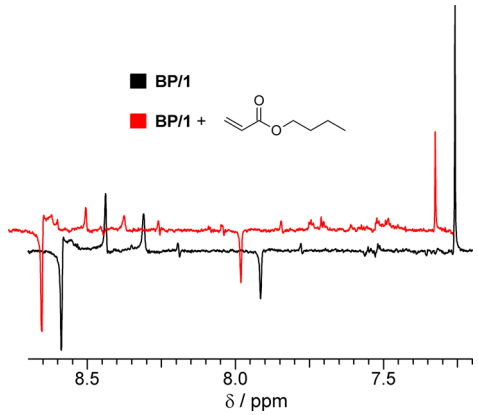


**Figure 12.** Zoom-in of the $^1$H CINDP spectrum of the initiator system **BP**/**1** and the same with the addition of butyl acrylate (spectrum horizontally shifted).

parent compound and its isomer are not affected by the addition of quencher (the monomer). This reveals that the formation of "cage" products is hardly influenced by the polymerization process. The clearly diminished intensity of the peaks corresponding to "escape" products **11**−**13** shows that phenyl radical **7** adds to the acrylates. Consequently all products formed at longer time scales from **7** are outcompeted by the monomer, which is present at much higher concentration compared to photoinitiator radicals. There was no effect seen on the two minor peaks at $\delta$ = 7.89 and 8.30 ppm (compare above), which are attributed to compounds **9** and **10**. Therefore, the CIDNP spectra reflect that the iminyl radical is not reactive toward the acrylate. This behavior of the two radicals **5** and **6** is in agreement with the TR-EPR results above.

The same experiment performed with ***t*-BAM** gave comparable relative intensities of the different signals. Therefore, one can expect to generalize the results for all acrylates. Furthermore, the reaction was performed with styrene as monomer, but the CIDNP spectra only gave very small signals compared to noise. This is attributed to the ability of styrene to act as a quencher of the **BP** triplet[44] while the oxime benzoate itself is not able to efficiently generate radicals under irradiation.[13,14]


dx.doi.org/10.1021/ma301959n | *Macromolecules* 2012, 45, 8648−8657

**Photoreactivity of 1 in the Presence of Sensitizers.** Preliminary experiments[19] have indicated that 4-methyl benzophenone **A** is an efficient sensitizer for **1**. To establish the range of suitable sensitizers, **A**–**C** in combination with **1** were tested.

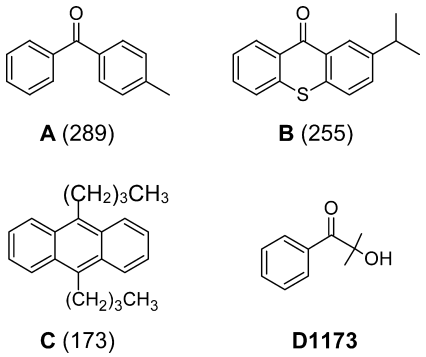


**Figure 13.** Reference initiator **D1173** and sensitizers **A**–**C**. The triplet energies of **A**–**C** are given in parentheses (in kJ $mol^{-1}$).[45]

Photo-DSC provides insights into the overall performance of polymerizing systems. Here the parameter $t_{max}$, the time needed to reach the maximum heat of polymerization, comprises effects which can be traced back to the efficiency of the photoinitiator. A comparison of $t_{max}$ values for selected sensitizer/initiator combinations for the polymerization of **HDDA** (1,6-hexanediol diacrylate) is shown in Figure 14. Sensitizer **C** does not reveal

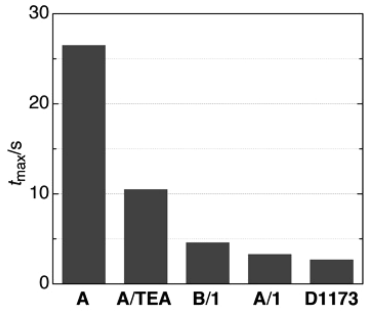


**Figure 14.** Photo-DSC data for oxime ester **1** with equimolar amounts of the sensitizers **A** and **B** as well as reference PI systems **A**/**TEA**, **A**, and **D1173**.

any effect, owing to its rather low triplet energy of 173 kJ $mol^{-1}$. The type II initiating system, **A** and triethanolamine (**TEA**), leads to $t_{max}$ = 10 s, and even **A** itself shows activity, but $t_{max}$ amounts to 26 s. This can be traced back to the hydrogen-abstraction ability of the corresponding excited triplet state. However, when sensitizers **A** and **B** (ITX, 2-isopropylthioxanthone) are utilized in combination with **1**, $t_{max}$ reaches the level of reference systems **A**/**TEA** and Darocur 1173 (**D1173**). Similar results were achieved for benzil and 2-ethylanthraquinone as sensitizer (data not shown).

## SUMMARY

In this study we have shown that benzaldoximes like *O*-benzoyl benzaldoxime ester **1** act as highly reactive type II photoinitiators when combined with an appropriate sensitizer. Reactivities similar to classical monomolecular compounds are possible, with the advantage that the spectral range of sensitivity can be easily tuned. It could be established that the radical initiation proceeds via triplet energy transfer from the sensitizer, followed by cleavage of the oxime N–O bond. In first instance an iminyl and a carboxylate radical are formed. The latter radical decarboxylates to give a carbon-centered radical, which induces polymerization. On the other hand, the iminyl radical does not contribute to the initiation at the observed time scale. Cis–trans photoisomerization at the C=N bond of the oxime moiety is observed in the CIDNP experiments.

In summary, the benzaldoxime-based initiators reveal efficient systems, which circumvent the complication of "back electron transfer" in type II systems. The reaction principles established here indicate pathways for the development of advanced phototriggers.

## ASSOCIATED CONTENT

### Supporting Information

NMR, CIDNP spectra, and reaction scheme of **BP**/**3**. This material is available free of charge via the Internet at http://pubs.acs.org.

## AUTHOR INFORMATION

### Corresponding Author

*E-mail: g.gescheidt-demner@tugraz.at.

### Present Address

[⊥]Department of Physical Chemistry, University of Geneva, Quai Ernest-Ansermet 30, 1211 Geneva, Switzerland.

### Notes

The authors declare no competing financial interest.

## ACKNOWLEDGMENTS

Financial support by the Austrian Science Fund FWF for this project, P19769-N14, is gratefully acknowledged.

## REFERENCES

(1) Yagci, Y.; Jockusch, S.; Turro, N. J. *Macromolecules* **2010**, *43*, 6245–6260.
(2) Fouassier, J. P.; Ruhlmann, D.; Graff, B.; Morlet-Savary, F.; Wieder, F. *Prog. Org. Coat.* **1995**, *25*, 235–271.
(3) Fouassier, J.-P. *Photoinitiation, Photopolymerization, and Photocuring: Fundamentals and Applications*; Hanser: Munich, 1995.
(4) Valderas, C.; Bertolotti, S.; Previtali, C. M.; Encinas, M. V. *J. Polym. Sci., Part A: Polym. Chem.* **2002**, *40*, 2888–2893.
(5) Moszner, N.; Salz, U. *Macromol. Mater. Eng.* **2007**, *292*, 245–271.
(6) Andrzejewska, E.; Zych-Tomkowiak, D.; Andrzejewski, M.; Hug, G. L.; Marciniak, B. *Macromolecules* **2006**, *39*, 3777–3785.
(7) Chatgilialoglu, C.; Lalevee, J. *Molecules* **2012**, *17*, 527–555.
(8) Jauk, S.; Liska, R. *Macromol. Rapid Commun.* **2005**, *26*, 1687–1692.
(9) Davidson, R. S.; Steiner, P. R. *J. Chem. Soc. C* **1971**, 1682–1689.
(10) Ullrich, G.; Burtscher, P.; Salz, U.; Moszner, N.; Liska, R. *J. Polym. Sci., Part A: Polym. Chem.* **2006**, *44*, 115–125.
(11) Griesser, M.; Dworak, C.; Jauk, S.; Hoefer, M.; Rosspeintner, A.; Grabner, G.; Liska, R.; Gescheidt, G. *Macromolecules* **2012**, *45*, 1737–1745.
(12) McCarroll, A. J.; Walton, J. C. *Chem. Commun.* **2000**, 351–352.
(13) McCarroll, A. J.; Walton, J. C. *J. Chem. Soc., Perkin Trans. 2* **2000**, 2399–2409.
(14) Yoshida, M.; Sakuragi, H.; Nishimura, T.; Ishikawa, S.; Tokumaru, K. *Chem. Lett.* **1975**, 1125–1130.
(15) McCarroll, A. J.; Walton, J. C. *J. Chem. Soc., Perkin Trans. 2* **2000**, 1868–1875.
(16) Kunimoto, K.; Oka, H.; Ohwa, M.; Tanabe, J.; Kura, H.; Birbaum, J. L. Ciba Specialty Chemicals Holding Inc., Switzerland. FR 2802528, 2001; 171 pp.

(17) Amat-Guerri, F.; Mallavia, R.; Sastre, R. *J. Photopolym. Sci. Technol.* **1995**, *8*, 205−232.
(18) Dietliker, K. In *A Compilation of Photoinitiators Commercially Available for UV Today*; SITA Technology Limited: London, 2002; p 129 ff.
(19) Dworak, C.; Liska, R. *J. Polym. Sci., Part A: Polym. Chem.* **2010**, *48*, 5865−5871.
(20) Baranyai, P.; Gangl, S.; Grabner, G.; Knapp, M.; Köhler, G.; Vidóczy, T. *Langmuir* **1999**, *15*, 7577−7584.
(21) Stoll, S.; Schweiger, A. *J. Magn. Reson.* **2006**, *178*, 42−55.
(22) Frisch, M. J.; Trucks, G. W.; Schlegel, H. B.; Scuseria, G. E.; Robb, M. A.; Cheeseman, J. R.; Montgomery, J. A.; Jr.; Vreven, T.; Kudin, K. N.; Burant, J. C.; Millam, J. M.; Iyengar, S. S.; Tomasi, J.; Barone, V.; Mennucci, B.; Cossi, M.; Scalmani, G.; Rega, N.; Petersson, G. A.; Nakatsuji, H.; Hada, M.; Ehara, M.; Toyota, K.; Fukuda, R.; Hasegawa, J.; Ishida, M.; Nakajima, T.; Honda, Y.; Kitao, O.; Nakai, H.; Klene, M.; Li, X.; Knox, J. E.; Hratchian, H. P.; Cross, J. B.; Bakken, V.; Adamo, C.; Jaramillo, J.; Gomperts, R.; Stratmann, R. E.; Yazyev, O.; Austin, A. J.; Cammi, R.; Pomelli, C.; Ochterski, J. W.; Ayala, P. Y.; Morokuma, K.; Voth, G. A.; Salvador, P.; Dannenberg, J. J.; Zakrzewski, V. G.; Dapprich, S.; Daniels, A. D.; Strain, M. C.; Farkas, O.; Malick, D. K.; Rabuck, A. D.; Raghavachari, K.; Foresman, J. B.; Ortiz, J. V.; Cui, Q.; Baboul, A. G.; Clifford, S.; Cioslowski, J.; Stefanov, B. B.; Liu, G.; Liashenko, A.; Piskorz, P.; Komaromi, I.; Martin, R. L.; Fox, D. J.; Keith, T.; Al-Laham, M. A.; Peng, C. Y.; Nanayakkara, A.; Challacombe, M.; Gill, P. M. W.; Johnson, B.; Chen, W.; Wong, M. W.; Gonzalez, C.; Pople, J. A. *Gaussian 03, Revision E.01*; Gaussian, Inc.: Wallingford, CT, 2004.
(23) Becke, A. D. *J. Chem. Phys.* **1993**, *98*, 5648.
(24) Stephens, P. J.; Devlin, F. J.; Chabalowski, C. F.; Frisch, M. J. *J. Phys. Chem.* **1994**, *98*, 11623−11627.
(25) Schaefer, A.; Huber, C.; Ahlrichs, R. *J. Chem. Phys.* **1994**, *100*, 5829−5835.
(26) Ramamurthy, V.; Turro, N. J.; Scaiano, J. C. *Modern Molecular Photochemistry of Organic Molecules*; University Science Publishers: New York, 2010.
(27) Lalevee, J.; Allonas, X.; Fouassier, J. P.; Tachi, H.; Izumitani, A.; Shirai, M.; Tsunooka, M. *J. Photochem. Photobiol., A* **2002**, *151*, 27−37.
(28) Chateauneuf, J.; Lusztyk, J.; Ingold, K. U. *J. Am. Chem. Soc.* **1988**, *110*, 2886−2893.
(29) Chateauneuf, J.; Lusztyk, J.; Ingold, K. U. *J. Am. Chem. Soc.* **1988**, *110*, 2877−2885.
(30) Wang, J.; Tateno, T.; Sakuragi, H.; Tokumaru, K. *J. Photochem. Photobiol., A* **1995**, *92*, 53−59.
(31) Wang, J.; Itoh, H.; Tsuchiya, M.; Tokumaru, K.; Sakuragi, H. *Tetrahedron* **1995**, *51*, 11967−11978.
(32) Gatlik, I.; Rzadek, P.; Gescheidt, G.; Rist, G.; Hellrung, B.; Wirz, J.; Dietliker, K.; Hug, G.; Kunz, M.; Wolf, J.-P. *J. Am. Chem. Soc.* **1999**, *121*, 8332−8336.
(33) Rosspeintner, A.; Griesser, M.; Pucher, N.; Iskra, K.; Liska, R.; Gescheidt, G. *Macromolecules* **2009**, *42*, 8034−8038.
(34) Dietliker, K.; Broillet, S.; Hellrung, B.; Rzadek, P.; Rist, G.; Wirz, J.; Neshchadin, D.; Gescheidt, G. *Helv. Chim. Acta* **2006**, *89*, 2211−2225.
(35) Griesser, M.; Neshchadin, D.; Dietliker, K.; Moszner, N.; Liska, R.; Gescheidt, G. *Angew. Chem., Int. Ed.* **2009**, *48*, 9359−9361.
(36) Adrian, F. J. *Res. Chem. Intermed.* **1991**, *16*, 99−125.
(37) Zemel, H.; Fessenden, R. W. *J. Phys. Chem.* **1975**, *79*, 1419−1427.
(38) Fischer, H.; Radom, L. *Angew. Chem., Int. Ed.* **2001**, *40*, 1340−1371.
(39) Vacek, K.; Geimer, J.; Beckert, D.; Mehnert, R. *J. Chem. Soc., Perkin Trans. 2* **1999**, 2469−2471.
(40) Kaptein, R. *J. Chem. Soc., Chem. Commun.* **1971**, 732−733.
(41) Pejkovic-Tadic, I.; Hranisavljevic-Jakovljevic, M.; Nesic, S.; Pascual, C.; Simon, W. *Helv. Chim. Acta* **1965**, *48*, 1157−1160.
(42) Bjoergo, J.; Boyd, D. R.; Watson, C. G.; Jennings, W. B. *Tetrahedron Lett.* **1972**, 1747−1750.
(43) Tori, K.; Otsuru, M.; Kubota, T. *Bull. Chem. Soc. Jpn.* **1966**, *39*, 1089.
(44) Kuhlmann, R.; Schnabel, W. *Polymer* **1976**, *17*, 419−422.
(45) Murov, S. L.; Hug, G. L.; Carmichael, I. *Handbook of Photochemistry*, 2nd ed.; M. Dekker: New York, 1993.